Reducing EMI through shielding enclosure perforations employing lossy materials: FDTD modeling and experiments

M. Li, S. Radu, J. Nuebel*
J. L. Drewniak, T. H. Hubing, T. P. VanDoren
Electromagnetic Compatibility Laboratory
Department of Electrical Engineering
University of Missouri at Rolla
Rolla, MO 65409

* Sun Microsystems, Inc.
2550 Garcia Avenue
Mountain View, CA 94043-1100

Abstract

A lossy material is employed to reduce EMI from slots and apertures that results when interior sources couple to perforations in the shielding enclosure of a Sun S-1000 server. A specially designed rectangular enclosure with a slot is also studied experimentally and with finite-difference time-domain (FDTD) simulations. The results for both the S-1000 and the simple rectangular enclosure indicate that a lossy material can be effective in reducing the Qs of cavity mode resonances and resonances introduced by the slot, therefore reducing the radiation through the slots and apertures.

1 Introduction

The integrity of shielding enclosures is compromised by slots and apertures for heat dissipation, CD-ROMs, I/O cable penetration, and plate-covered unused connector ports, among other possibilities. Radiation from slots and apertures in conducting enclosures excited by interior sources is of great concern in meeting FCC radiated EMI limits. The radiation from enclosures through apertures has previously been studied numerically [1], though reported design approaches for reducing the radiation are limited.

Results presented in this paper indicate that numerical modeling of enclosure designs can aid in developing enclosure guidelines. The application of a lossy material in a simple rectangular enclosure fed with a wire probe was investigated. With appropriate modeling of the essential features such as the source, load, and loss, the FDTD simulated results of the delivered power agreed with the measurements. The simulated and measured results for the simple rectangular cavity show that the employment of a lossy material can reduce the Qs of the cavity mode resonances and resonances due to the slot. Two-port S-parameter measurements of the simple rectangular enclosure showed a lossy material bonded to one of the enclosure walls was effective in reducing EMI.

An S-1000 server was also investigated. Radiated EMI measurements on a functioning S-1000 showed that the lossy material could be effective in reducing EMI. However, the location of the lossy material and the EMI noise source at the PCB level is important to this effect. The potential for reducing EMI by putting lossy material on the enclosure walls is demonstrated herein through FDTD simulations and experiments. However, further work is necessary both in identifying and modeling the EMI noise source at the PCB to minimize cost in a practical design.

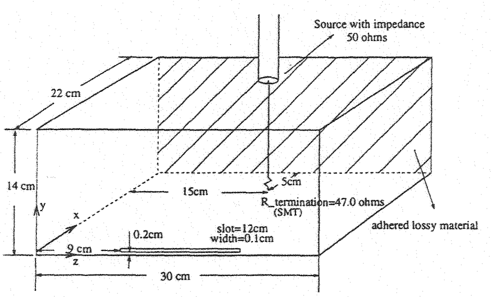

Figure 1: The geometry of the specially designed rectangular enclosure.

2 FDTD and Experimental Results

A rectangular enclosure with a thin slot near an edge was designed to study EMI through slots. The geometry of the experimental conducting enclosure is shown in Figure 1. The cavity was fed with a 50 Ω coaxial cable probe through a type-N bulkhead connector, which was peripherally bonded to the cavity. The center conductor of the probe was extended to span the width of the cavity with a 0.16 cm diameter wire, and terminated on the opposite cavity wall with a 1206 package size surface-mount (SMT) 47 Ω resistor stood on end and soldered to a $1.5'' \times 1.5''$ square of conductive adhesive copper tape. The feed probe was located at $x = 17$ cm, $y = 14$ cm, and $z = 15$ cm.

The cavity was constructed of 5 pieces of 0.635 cm thick aluminum, and one plate of 0.05 cm thick aluminum for the face containing the slot. A slot of width $w_s = 0.1$ cm ($\frac{w_s}{\delta y} = 0.2$) and length of 12 cm was located 0.25 $cm = \frac{1}{2}\delta y$ from the center of the slot to the bottom edge, where δy is the mesh dimension along the y-axis. The inside dimensions of the enclosure were 22 $cm \times$ 14 $cm \times$ 30 cm. One-inch copper tape with conductive adhesive was used to electromagnetically seal the seams. Two layers of lossy dielectric material with $R_\square = 1500\Omega/\square$ and thickness $d = 0.4$ cm (conductivity $\sigma = \frac{1}{R_\square d} = 0.00167$ S/cm) were employed on the interior wall $x = 22$ cm.

Two-port S-parameters were measured in a semi-anechoic chamber, where the enclosure under test was connected to Port 1 of a Wiltron 37247A network analyzer, and a horn antenna as the receiver was connected to Port 2 of the network analyzer. The network analyzer was placed outside the semi-anechoic room to measure the reflection coefficient $|S_{11}|$, from which the real power delivered by the source normalized to the source voltage was calculated as

$$P = \frac{1}{8Z_0}(1 - |S_{11}|^2). \tag{1}$$

The transmission coefficient $|S_{21}|$, which is related to the radiated power was also measured. The antenna factor of the receiving horn was not included in the calibration procedure, and the $|S_{21}|$ results were only relative measurements of improvements with the lossy material.

A cell size of 1.0 $cm \times$ 0.5 $cm \times$ 1.0 cm was employed in the FDTD simulations, where finer discretization along the y direction was used in order to better model the spatial extent of the SMT load resistor. The feed probe was modeled employing a quasi-static approach that modifies the magnetic field circling the wire [2]. The feed source was modeled by a simple gap voltage source V_s with a 50-Ω source resistance incorporated into a single cell at the feed point. The magnetic fields circling the source were modeled in the same fashion as a thin wire to give the cross-section of the source specified physical dimensions [3]. A magnetic frill type source, which may be more accurate in modeling the connector, was also investigated, but yielded little improvement over the wide gap type source [9]. The resistor was modeled as a lumped element using a subcellular algorithm [4]. The width of the SMT is approximately that of the feed probe diameter and the physical cross-section dimensions were modeled with the same diameter as that of the feed probe by modifying the magnetic field components circling the SMT in the same fashion as for the source. The slot was modeled with a capacitive thin-slot subcellular algorithm to avoid a small mesh dimension [5], and perfectly-matched-layer (PML) absorbing boundary conditions were employed for the 3D simulations [6]. The lossy material was simply modeled by a one-cell layer of conducting material with conductivity $\sigma = 0.00167\ S/cm$. For the electric field components inside the conducting layer, the conductivity $\sigma = 0.00167\ S/cm$ was employed, while the conductivity $\sigma = \frac{0.00167}{2}\ S/cm$ was employed for the components in the interface of conducting layer and free space [7].

A sinusoidally modulated Gaussian pulse was employed as the excitation. The source voltage as a function of time t was

$$V_s(t) = e^{-\alpha^2(t-t_0)^2} cos[2\pi f_0(t-t_0)], \qquad (2)$$

where $f_0 = \frac{f_{upper}+f_{lower}}{2}$ is the center frequency (f_{lower} is the starting frequency and f_{upper} is the stopping frequency), and α and t_0 are

$$\alpha = \frac{\pi(f_{upper} - f_{lower})}{\sqrt{-ln(b_{BW})}}, \qquad (3)$$

$$t_0 = \frac{1}{\alpha}\sqrt{-ln(b_t)}, \qquad (4)$$

where b_{BW} is the minimum pulse level which is unaffected by computational noise, and b_t is the maximum allowable pulse level at $t = 0$. b_{BW} and b_t were set to be 0.0001 and 0.001, respectively, so that the temporal pulse was greater than two orders of magnitude below the maximum at the beginning and end of the pulse. A time step of 8.3333 ps was employed. The time-history of the voltage V_0 across the source and source impedance, and the current I_0 through the source were stored, and an FFT was employed to calculate frequency-domain quantities. A total of 20,000 time steps was required for a good resolution in the frequency domain. In simulations with frequency bands containing very high Q resonances, e.g., 1.36 GHz in Figure 2 for the case without the lossy material, an additional 20,000 time steps, or 40,000 total were required in order for the stored energy to decay and minimize ringing. The computed real power delivered by the source normalized to the source voltage was calculated as

$$P_{FDTD} = \frac{1}{2|V_s|^2} Re(\hat{V}_0 \times \hat{I}_0^*). \qquad (5)$$

The measured and simulated delivered power are shown in Figure 2 for the configuration in Figure 1 with the lossy material on the interior face $x = 22\ cm$, and without the lossy material. The available power from the source was 2.5 mW. The agreement between measurements and simulations is generally good. The measured and simulated results without the lossy material agree well over the entire frequency range considered. There is a slight discrepancy at 1.24 GHz which is the slot half-wave resonance. This shift to higher frequency for the FDTD results as compared to the measured results is due to the particular thin-slot subcellular algorithm employed. The agreement is nearly exact, to within measurement and simulation error if a more sophisticated thin-slot algorithm is used [9]. Since the feed probe was along the y direction, the y-component of the electric field was excited, while the y-component of the magnetic field was suppressed, i.e., only TM_y cavity modes were excited by the feed probe. For the configuration without the lossy material, the TM_y101 cavity mode is at 0.89 GHz. Resonances at 1.36 GHz and 1.44 GHz correspond to the TM_y111 and TM_y201 modes, respectively. The resonances at 1.12 GHz and 1.24 GHz are due to the slot. Measurements indicated that the resonance at 1.53 GHz was due to the slot as well. Calculations from the FDTD simulations of the power dissipated in the load resistor showed that most of the power delivered by source was radiated through slot at this resonance. The resonances at 1.12 GHz and 1.53 GHz result from interaction of the slot with the feed probe or cavity, and tuning of the reactance [8]. Calculations from FDTD simulations of the power dissipated in the load resistor and total power showed that 28%, 60%, and 89% of the delivered power was radiated through the slot at 1.12 GHz, 1.24 GHz, and 1.53 GHz, respectively. For the configuration with the lossy material, the TM_y101 cavity mode was virtually unaffected, and the feed probe TEM mode at 1.08 GHz [9] was shifted down by 2.5%. The resonances due to the slot at 1.12 GHz and 1.24 GHz were shifted with an increase in the radiated power at 1.20 GHz. The high-Q TM_y111 cavity mode at 1.36 GHz was greatly reduced, and the Q of the TM_y201 cavity mode at 1.44 GHz was also reduced. The significant discrepancy between the FDTD and measured results with the lossy material at the resonance at 1.53 GHz may be due

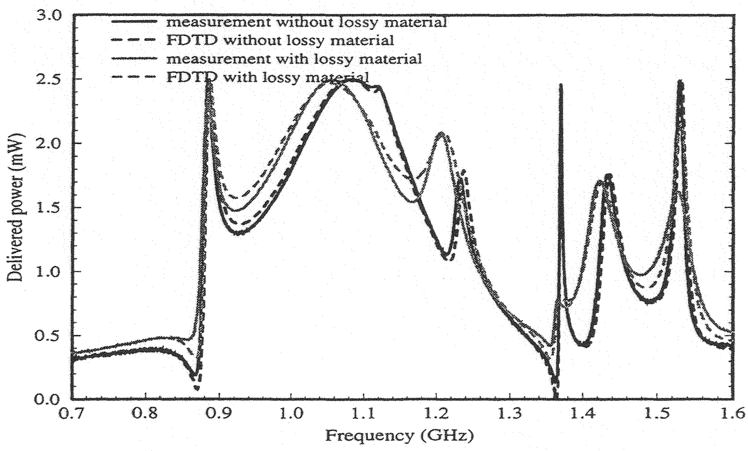

Figure 2: Measured and simulated delivered power to the specially designed rectangular enclosure with and without a lossy material.

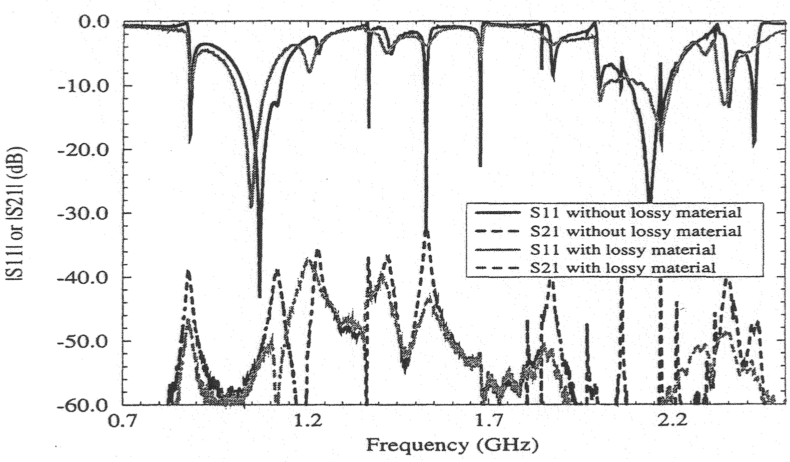

Figure 3: The two-port measured results for the simple rectangular enclosure with and without the lossy material.

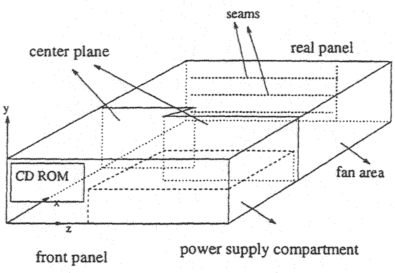

Figure 4: The geometry of the S-1000 enclosure.

to a frequency dependence in the conductivity of the lossy material.

Two-port measured results ($|S_{11}|$ and $|S_{21}|$) for the simple rectangular cavity with and without the lossy material are shown in Figure 3. The $|S_{11}|$ measurements were used for comparison with FDTD simulations in Figure 2. For the configuration without the lossy material, the radiation at the cavity modes is as significant as the radiation at the resonances due to the slot. The effect of the lossy material in decreasing the Qs of resonances is evident in the measured $|S_{11}|$, and reflected in reduced radiation in $|S_{21}|$, e.g., the TM_y101 at 0.89 GHz, the TM_y111 at 1.36 GHz, the TM_y201 at 1.44 GHz, and the resonance at 1.53 GHz. However, a resonance and a corresponding increase in radiation were measured at 1.20 GHz, where the two resonances due to the slot at 1.10 GHz and 1.24 GHz for the situation without the lossy material may have shifted and broadened to produce the resonance at 1.20 GHz.

The potential for reducing EMI through a judicious use of lossy material on enclosure walls was investigated in a functioning Sun S-1000 high-speed server design. A representation of the Sun S-1000 enclosure partitioned into front and back portions by a center plane is shown in Figure 4. One motherboard with a single CPU module was in the back portion, while a CD ROM, a controller card, and a power supply were in the front portion. Loss was introduced in the enclosure by adhering the lossy material to the interior top, bottom, and back faces, as well as the center plane. EMI from the functioning S-1000 production design was measured in a shielded room with a Tektronix 2712 Spectrum Analyzer, using a log periodical dipole array as the receiving antenna. The primary radiators for the design above 500 MHz were slots and apertures as determined from radiated measurements. The only attached cable during the measurement procedures was the power chord.

Radiated EMI measurements for a functioning S-1000 system with and without the lossy material on the previously indicated walls are shown in Figure 5. At frequencies above 500 MHz, the decrease in radiated EMI was $5 - 20$ dB for most CPU harmonics (60 MHz fundamental frequency), e.g., 5 dB at 900 MHz, 14 dB at 1320 MHz, and 20 dB at 1440 MHz, while at frequencies below 500 MHz, there was no significant effect. The radiation increased by 5dB at 600 MHz and 700 MHz. The position of the lossy material was also important and the employment of the lossy material on the center plane was most significant.

3 Summary and Conclusion

FDTD modeling of an interior-excited simple rectangular enclosure with a thin slot near an edge was compared with experimental results. The agreement was good for configurations with and without a lossy material on one enclosure wall. The lossy material was effective in reducing the Qs of the cavity mode resonances and resonances due to the slot, and reducing EMI through the slot. The potential of a lossy material in reducing EMI was also demonstrated in a functioning server system. However, further work is necessary in determing the optimal amount of loss in the material, the type of lossy material—dielectric or magnetic, and a method for selecting the optimum locations for loss The agreement between the simulated and measured results indicates that these issues can be explored relying on FDTD simulations, with fewer, more selective experiments for corroboration.

4 Acknowledgments

The authors gratefully acknowledge assistance from Yun Ji, and Wei Cui in portions of the measure-

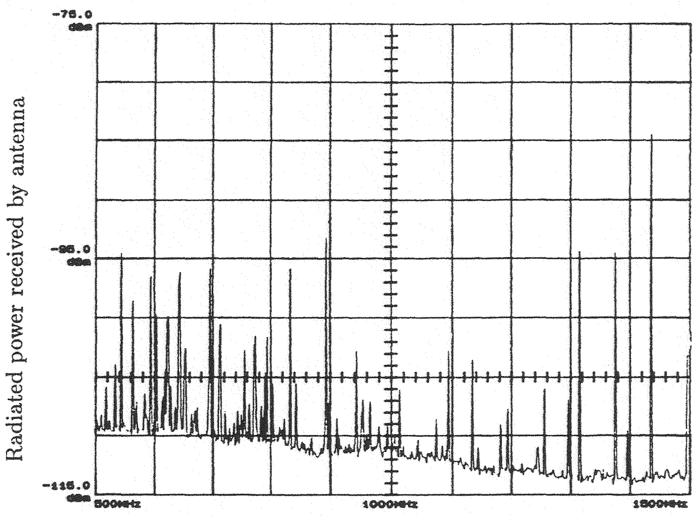

(a)

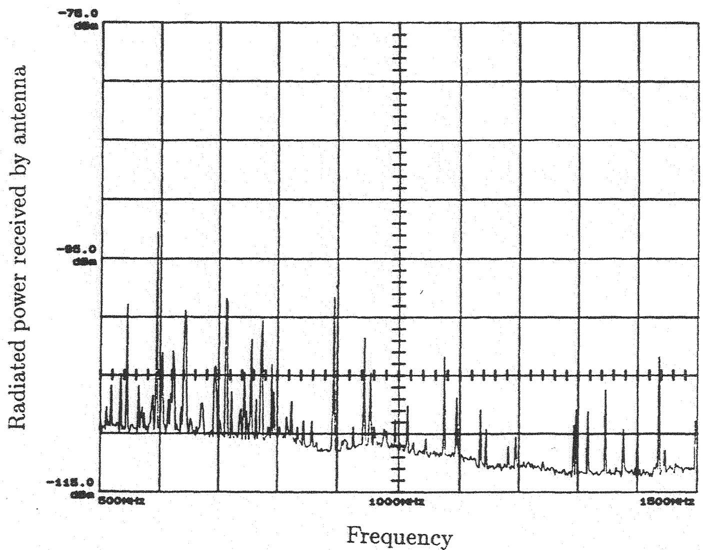

(b)

Figure 5: Radiated EMI measurements from a functioning S-1000 system (500 MHz — 1500 MHz) (a) without the lossy material, and (b) with lossy material.

ments.

References

[1] H. Moheb, L. Shafai and J. Shaker, "Numerical solution of radiation from single and multiple arbitrary apertures backed by a cavity", *IEEE Antennas and Propagat. Symposium, 1992 Digest*, vol. 1, pp. 61-64, 1992.

[2] A. Taflove, *Computational Electrodynamics.* Artech House; Boston, 1995.

[3] David M. Hockanson, James L. Drewinak, Todd H. Hubing and Thomas P. Van Doren, "FDTD modeling of common-mode radiation from cables," *IEEE Trans. Electromagn. Compat.*, vol. 38, pp. 376-387, August 1996.

[4] Yuh-Sheng Tsuei, A. C. Cangellaris and J. L. Prince, "Rigorous electromagnetic modeling of chip-to-package (first-level) interconnections," *IEEE Transactions on Components, Hybrids, and Manufacturing Technology,* vol. 16, pp.876-882, December 1993.

[5] J. Gilbert and R. Holland, "Implementation of the thin-slot formalism in the finite-difference EMP code THREDII," *IEEE Trans. Nuclear Sci.*, vol. NS-28, pp. 4269-4274, December 1981.

[6] J. P. Berenger, "Perfectly matched layer for the absorption of electromagnetic waves," *Journal of Computational Physics*, vol. 114, pp. 185-200, October 1994.

[7] D. M. Hockanson, *The Finite Difference Time Domain Method and Applications in Electromagnetic Compatibility*, M. S. Thesis, University of Missouri-Rolla, 1994.

[8] Chang-Hong Liang and D. K. Cheng, "Electromagnetic fields coupled into a cavity with a slot-aperture under resonant conditions," *IEEE Trans. Antennas Propagat.*, vol. AP-30, pp. 664-672, July 1982.

[9] M. Li, *Investigation of Electromagnetic Interference Through Slots in Shielding Enclosures: Finite-Difference Time-Domain Simulations and Experiments*, M. S. Thesis, University of Missouri-Rolla, 1996.